J Neurophysiol 107: 692–703, 2012.
First published November 2, 2011; doi:10.1152/jn.00281.2011.

D_2-like dopamine receptors differentially regulate unitary IPSCs depending on presynaptic GABAergic neuron subtypes in rat nucleus accumbens shell

Shuntaro Kohnomi,[1] Noriaki Koshikawa,[1,2] and Masayuki Kobayashi[1,2,3]

[1]*Department of Pharmacology and* [2]*Division of Oral and Craniomaxillofacial Research, Dental Research Center, Nihon University School of Dentistry, Tokyo; and* [3]*RIKEN Center for Molecular Imaging Science, Minatojima-minamimachi, Chuo-ku, Kobe, Japan*

Submitted 30 March 2011; accepted in final form 31 October 2011

Kohnomi S, Koshikawa N, Kobayashi M. D_2-like dopamine receptors differentially regulate unitary IPSCs depending on presynaptic GABAergic neuron subtypes in rat nucleus accumbens shell. *J Neurophysiol* 107: 692–703, 2012. First published November 2, 2011; doi:10.1152/jn.00281.2011.—In the nucleus accumbens (NAc), a medium spiny (MS) neuron receives GABAergic inputs from two major sources: fast-spiking (FS) neurons and other, adjacent MS neurons. These two types of inhibitory synapses are considered to play different roles in output activities, i.e., FS→MS connections suppress output from the NAc whereas MS→MS connections contribute to lateral inhibition. In the present study, we focused on the electrophysiological properties of unitary inhibitory postsynaptic currents (uIPSCs) obtained from MS→MS connections and FS→MS connections and examined the effects of quinpirole, a dopamine D_2-like receptor agonist, on uIPSCs with multiple whole cell patch-clamp recording. Application of quinpirole (1 μM) reliably suppressed the amplitude of uIPSCs by 29.6% in MS→MS connections, with increases in paired-pulse ratio and failure rate. The suppressive effects of quinpirole on uIPSCs were mimicked by 1 μM PD128907, a $D_{2/3}$ receptor agonist, whereas quinpirole-induced suppression of uISPCs was blocked by preapplication of 1 μM sulpiride or 10 μM nafadotride, both $D_{2/3}$ receptor antagonists. On the other hand, quinpirole (1 μM) had divergent effects on FS→MS connections, i.e., quinpirole increased uIPSC amplitude in 38.1% of FS→MS connections and 23.8% of FS→MS connections were suppressed by quinpirole. Analysis of coefficient of variation in uIPSC amplitude implied the involvement of presynaptic mechanisms in quinpirole-induced effects on uIPSCs. These results suggest that activation of D_2-like receptors facilitates outputs from MS neurons in the NAc by reducing lateral inhibition during a dormant period of FS neuron activities.

medium spiny neuron; fast-spiking neuron; quinpirole; whole cell patch clamp

THE NUCLEUS ACCUMBENS (NAc), a rostroventromedial extension of the striatum, plays a critical role in reward-related behaviors, drug abuse, psychosis, learning, and motor control (Cools et al. 1995; Di Chiara 2002; Koshikawa et al. 1990; Nicola 2007; Sharp et al. 1987). Such physiological and pathological functions are considered to be regulated by dopamine released from dopaminergic terminals located in the ventral tegmental area (Morgane et al. 2005). Indeed, the NAc contains dopamine D_1-like (D_1 and D_5) and D_2-like (D_2, D_3, and D_4) receptors (Lu et al. 1998; Sibley et al. 1993). This area is also known to receive glutamatergic projections from a variety of limbic areas such as the prefrontal cortex, hippocampus, and basolateral amygdala (Groenewegen et al. 1991; Pennartz et al. 1994; Shinonaga et al. 1994). In vitro whole cell patch-clamp recordings from medium spiny (MS) neurons have demonstrated that dopamine suppresses these excitatory synaptic inputs to MS neurons via presynaptic mechanisms and that these suppressive dopaminergic effects of dopamine are mediated by D_1-like receptors (Nicola et al. 1996; Nicola and Malenka 1997; Pennartz et al. 1992).

The striatum includes abundant GABAergic neurons such as MS, fast-spiking (FS), and persistent and low-threshold spike (PLTS) neurons in addition to cholinergic neurons (Kawaguchi et al. 1995). Similar to the striatum, principal cells in the NAc are MS neurons, which constitute the majority (90–95%) population and send their axons to the ventral pallidum and midbrain dopaminergic cell areas, including the ventral tegmental area, substantia nigra pars compacta, and retrorubral field (Groenewegen et al. 1991). MS neurons receive inhibitory GABAergic inputs from at least two sources. Parvalbumin-immunopositive cells, which receive powerful glutamatergic inputs from the cerebral cortex, are the main inhibitory interneurons projecting to MS neurons (Kawaguchi et al. 1995). Anatomical features of parvalbumin-immunopositive cells are their dense arborization of local axon collaterals innervating NAc neurons, including MS cells. Parvalbumin-immunopositive cells are classified physiologically as FS neurons characterized by their extremely high frequency of repetitive spike firing without adaptation, short spike duration, and lower input resistance (Kawaguchi 1993; Taverna et al. 2007). Considering these morphological and physiological features, FS neurons potently suppress MS neuron activity in the NAc. Another neuron subtype projecting to MS neurons is the MS neuron itself. MS neurons are functionally connected each other and form a lateral inhibition network in the NAc (Pennartz and Kitai 1991; Taverna et al. 2004) as well as striatum (Czubayko and Plenz 2002; Guzmán et al. 2003; Koós and Tepper 1999; Tepper et al. 2004, 2008). Interestingly, recurrent collateral connections in the striatum were reported to be disrupted in rodent models of Parkinson's disease (Taverna et al. 2008), indicating that these MS-MS connections are functionally important.

In the NAc, several patch-clamp studies have revealed that dopamine suppresses extracellular stimulation-induced inhibitory postsynaptic potentials (IPSPs)/inhibitory postsynaptic currents (IPSCs), which are likely to originate from axon collaterals of MS neurons (Pennartz and Kitai 1991; Taverna et al. 2004), and these suppressive effects of dopamine are presumed to be mediated through D_1-like receptors (Hjelmstad 2004; Nicola and Malenka 1997; Taverna et al. 2005). Al-

Address for reprint requests and other correspondence: M. Kobayashi, Dept. of Pharmacology, Nihon Univ. School of Dentistry, 1-8-13 Kanda-Surugadai, Chiyoda-ku, Tokyo 101-8310, Japan (e-mail:kobayashi-ms@dent.nihon-u.ac.jp).

though D_2-like receptor antagonists are often used clinically to treat neuropsychiatric diseases such as schizophrenia, which indicates the critical importance of D_2-like receptors in higher brain functions, the mechanisms of their precise regulation of IPSCs elicited by specific GABAergic neuron subtypes (e.g., FS→MS connections) are still an open issue.

To clarify comprehensively the dopaminergic regulation of inhibitory synaptic transmission in the NAc, it is necessary to discriminate the source of GABAergic inputs. The NAc is divided into core and shell with respect to anatomy (Heimer et al. 1991; Jongen-Rêlo et al. 1994; Zahm and Brog 1992), receptor density (Deutch and Cameron 1992), and electrophysiology (Pennartz et al. 1992). Abundant data on D_2 receptors have been accumulated in reports that emphasize the importance of the shell, but not the core, in dyskinesia (Cools et al. 1995; Koshikawa et al. 1996; Prinssen et al. 1994). We therefore focused on the roles of D_2-like receptors in inhibitory synaptic transmission from FS to MS (FS→MS) and MS to MS (MS→MS) neurons by multiple whole cell patch-clamp recordings in the NAc shell.

MATERIALS AND METHODS

All experiments were performed in accordance with the National Institutes of Health *Guide for the Care and Use of Laboratory Animals* and were approved by the Institutional Animal Care and Use Committee of Nihon University School of Dentistry. All efforts were made to minimize the number of animals used and their suffering.

Slice preparations. The techniques for preparing and maintaining rat brain slices in vitro were similar to those described previously (Koyanagi et al. 2010; Yamamoto et al. 2010). Briefly, Wistar rats of either sex aged postnatal days 20–30 were used for brain slice preparations. Rats were deeply anesthetized with pentobarbital sodium (75 mg/kg ip) and decapitated. Tissue blocks including the NAc were rapidly removed and stored for 2 min in ice-cold modified artificial cerebrospinal fluid (ACSF) (in mM): 230 sucrose, 2.5 KCl, 10 $MgSO_4$, 1.25 NaH_2PO_4, 26 $NaHCO_3$, 0.5 $CaCl_2$, and 10 D-glucose. Coronal slices were cut at 350-μm thickness with a microslicer (Linearslicer Pro 7, Dosaka EM, Kyoto, Japan). Slices were incubated at 32°C for 20 min in a submersion-type holding chamber that contained 50% modified ACSF and 50% normal ACSF (pH 7.35–7.40). Normal ACSF contained (in mM) 126 NaCl, 3 KCl, 2 $MgSO_4$, 1.25 NaH_2PO_4, 26 $NaHCO_3$, 2.0 $CaCl_2$, and 10 D-glucose. Modified and normal ACSF were continuously aerated with a mixture of 95% O_2-5% CO_2. Slices were then placed in normal ACSF at 32°C for 1 h and thereafter maintained at room temperature until used for recording.

Cell identification and paired whole cell patch-clamp recording. The slices were transferred to a recording chamber that was perfused continuously with normal ACSF at a rate of 1.5–2.0 ml/min. Dual, triple, or quadruple whole cell patch-clamp recordings were obtained from MS neurons and/or FS cells identified in the shell of NAc by a microscope equipped with Nomarski optics (×40, Olympus BX51, Tokyo, Japan) and an infrared-sensitive video camera (Hamamatsu Photonics, Hamamatsu, Japan). The distance between MS/FS cells was <50 μm. Electrical signals were recorded by amplifiers (Axopatch 200B, Axoclamp 900A, and Multiclamp 700B, Axon Instruments, Foster City, CA), digitized (Digidata 1440A, Axon Instruments), observed online, and stored on a computer hard disk with software (Clampex 10, Axon Instruments). Membrane currents and potentials were low-pass filtered at 5–10 kHz and digitized at 20 kHz.

The composition of the pipette solution for recordings from MS and FS neurons was (in mM) 70 potassium gluconate, 70 KCl, 10 HEPES, 15 biocytin, 0.5 EGTA, 2 $MgCl_2$, 2 magnesium ATP, and 0.3 sodium GTP. The pipette solution had a pH of 7.3 and osmolarity of 300 mOsm. The liquid junction potentials for current-clamp and voltage-clamp recordings were −9 mV, and voltage was corrected accordingly. Thin-wall borosilicate patch electrodes (4–5 MΩ) were pulled on a Flaming-Brown micropipette puller (P-97, Sutter Instruments, Novato, CA).

Recordings were obtained at 30–31°C. Seal resistance was >5 GΩ, and only data obtained from electrodes with access resistance of 6–20 MΩ and <20% change during recordings were included in this study. Before unitary IPSC (uIPSC) recordings, voltage responses of presynaptic and postsynaptic cells were recorded by application of long hyperpolarizing and depolarizing current pulse (300–400 ms) injections to examine basic electrophysiological properties, including input resistance, single-spike kinetics, voltage-current relationship, and repetitive firing pattern and frequency. Short depolarizing double pulses (2 ms, 0.8–1.5 nA or 80 mV) with 25- to 50-ms interpulse interval were applied to presynaptic cells to induce action potentials/currents. In dual whole cell patch-clamp recordings, presynaptic cells were recorded under current-clamp conditions except for the case in which two neurons mutually connected. In triple or quadruple whole cell patch-clamp recordings, all cells were recorded under voltage-clamp conditions, because a presynaptic cell possibly received projections from another cell. In voltage-clamp recordings, all neurons were held at −80 mV. Voltage step pulses from −80 mV to 0 mV induced unclamped action potentials in presynaptic cells. To eliminate the excitatory glutamate inputs, the AMPA glutamate receptor antagonist 6,7-dinitroquinoxaline-2,3-dione (DNQX, 20 μM; Research Biochemicals International, Natick, MA) was added during uIPSC recording.

The following drugs were used in this study: bicuculline methiodide (Tocris Cookson, Bristol, UK), quinpirole hydrochloride (Sigma-Aldrich, St. Louis, MO), S-(−)-sulpiride (Sigma-Aldrich), nafadotride (Sigma-Aldrich), and PD128907 hydrochloride (Sigma-Aldrich). All drugs were added to the perfusing ACSF. DNQX, S-(−)-sulpiride, and nafadotride were dissolved with 0.1% DMSO in ACSF.

Data analysis. Clampfit (pClamp 10, Axon Instruments) was used for analyses of electrophysiological data. Input resistance was measured from slopes of least-squares regression lines fitted to voltage-current (*V–I*) curves measured at the peak voltage deflection (current pulse amplitude up to −100 pA). The amplitudes of the action potential and afterhyperpolarization (AHP) were measured from the action potential threshold. By application of depolarizing step current pulses (300–400 ms), rheobase was identified as the minimal current that consistently elicited an action potential. Repetitive firing was evaluated by measuring the maximal firing rate and slope of least-squares regression lines in a plot of the number of spikes versus the amplitude of injected current, i.e., the frequency-current (*F–I*) curve (up to ~400 pA).

Amplitudes of uIPSCs were measured as the difference between the peak postsynaptic currents and the baseline currents taken from a 2- to 3-ms time window close to the onset of the uIPSCs. Average amplitude, paired-pulse ratio (PPR) of the second to first uIPSC amplitude, coefficient of variation (CV), and failure rate of the first uIPSCs in control were calculated from 10 events just before drug application. For quantification of the drug effects on uIPSCs, the last 10 events recorded during the drug application were analyzed. uIPSC amplitude in the range of synaptic noise was taken as failure. Failure events were included for computation of uIPSC amplitude, PPR, and CV. The 20–80% rise time, 80–20% decay time, and onset latency of uIPSCs were measured from average traces, which were obtained from traces aligned to the peak of presynaptic action potentials. The decay phase from peak to baseline was fitted by a double exponential function (Origin version 8, Microcal Software, Northampton, MA, USA):

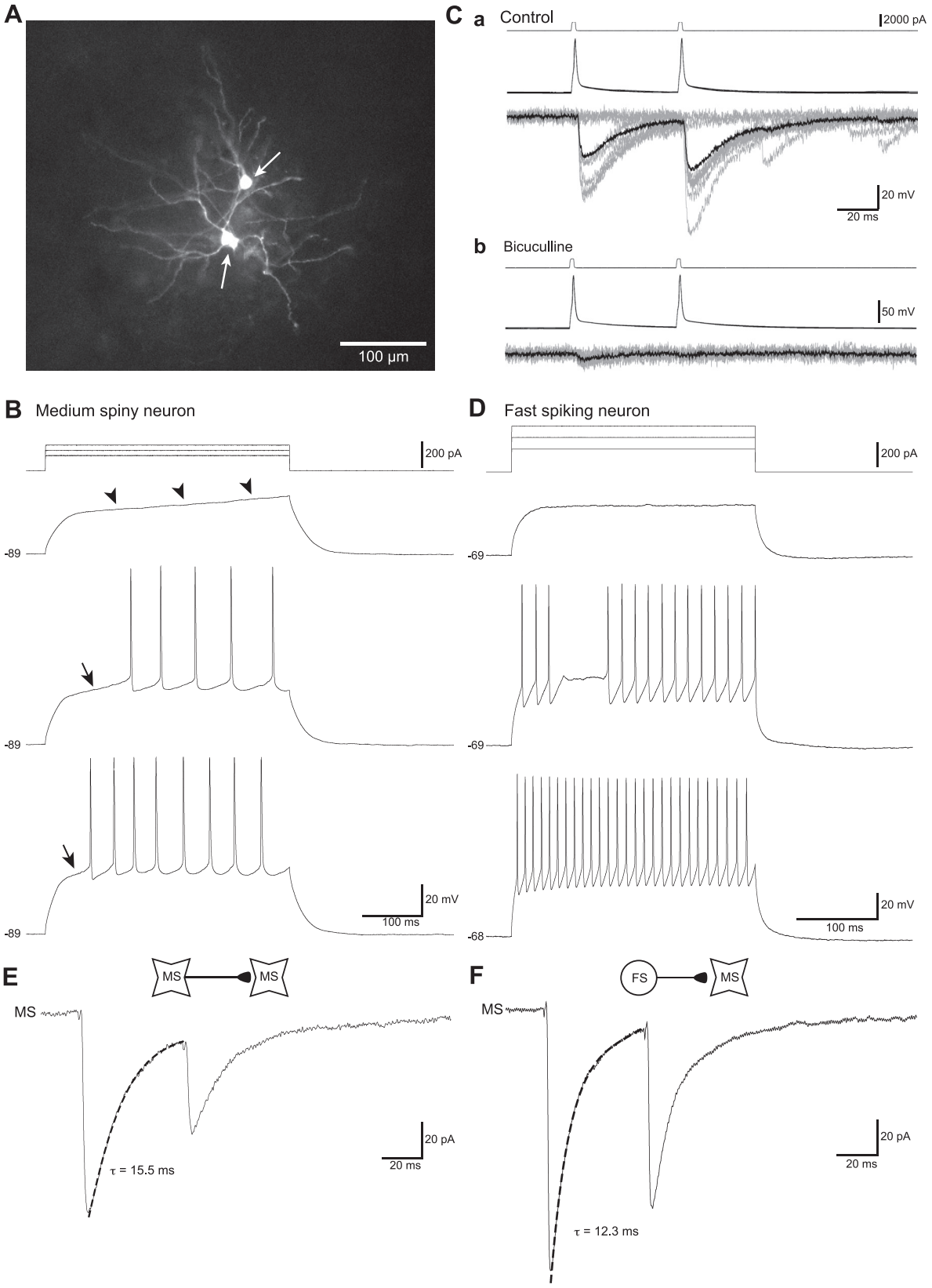

Table 1. *Intrinsic electrophysiological properties of MS and FS neurons*

	Medium Spiny Neuron	*n*	Fast-Spiking Neuron	*n*
V_m, mV	−82.8 ± 0.6	97	−81.7 ± 1.1	24
Input resistance, MΩ	258.5 ± 17.0	97	145.7 ± 19.6***	24
Action potential				
Threshold, mV	−48.0 ± 0.6	97	−48.4 ± 1.3	24
Amplitude, mV	73.6 ± 1.3	97	62.6 ± 2.7***	24
Half-duration, ms	1.42 ± 0.02	97	0.70 ± 0.04***	24
AHP amplitude, mV	6.7 ± 0.5	97	18.1 ± 1.7***	24
Rheobase, pA	118.0 ± 6.1	83	185.2 ± 19.8**	21
Repetitive firing				
Maximal firing rate, Hz	32.4 ± 1.2	81	86.2 ± 6.2***	21
F–I slope, Hz/pA	0.46 ± 0.03	83	0.79 ± 0.10**	21

Values are means ± SE. MS, medium spiny; FS, fast spiking; V_m, resting membrane potential; AHP, afterhyperpolarization; *F–I*, frequency-current. $^{**}P < 0.01$, $^{***}P < 0.001$, Student's *t*-test.

$$f(t) = A_{fast}\exp(-t/\tau_{fast}) + A_{slow}\exp(-t/\tau_{slow}) \quad (1)$$

where A_{fast} and A_{slow} are the amplitudes of fast and slow decay components, respectively, and τ_{fast} and τ_{slow} are their respective decay time constants. The weighted decay time constant (τ_w) was calculated with the following equation (Bacci et al. 2003; Kobayashi et al. 2008):

$$\tau_w = \left[(A_{fast}\tau_{fast}) + (A_{slow}\tau_{slow})\right]/(A_{fast} + A_{slow}) \quad (2)$$

Data are presented as means ± standard error (SE). The intrinsic electrophysiological properties of neurons and kinetics of uIPSCs were analyzed by Student's *t*-test. Comparisons of the uIPSC amplitude and PPR between control and drug application were conducted by paired *t*-test. Normality of these data sets was tested by Shapiro-Wilk normality test with software (SPSS version 12, Chicago, IL). Because the distribution of failure rate could not be fitted with a normal distribution, a nonparametric Wilcoxon test was applied for its comparison. Connection rates of MS→MS and FS→MS neurons were compared by χ^2-test. In each cell pair, Student's *t*-test was used to classify the drug-induced changes of uIPSC amplitude, i.e., facilitation, suppression, or no change. The level of $P < 0.05$ was adopted to indicate significance.

Histology. To visualize biocytin-labeled neurons after whole cell patch-clamp recording, slices were fixed and cryoprotected. Sections were processed by the ABC method (Vector Laboratories, Burlingame, CA), and fluorescence was visualized with Alexa 488-conjugated streptavidin (Molecular Probes, Eugene, OR). Slices were examined and imaged with a fluorescent microscope (BZ-9000, Keyence, Osaka, Japan). All chemicals, unless specified otherwise, were purchased from Sigma-Aldrich.

RESULTS

Whole cell patch-clamp recordings were performed in neurons in the NAc shell; neurons were randomly selected except for neurons with large somata that are considered to be cholinergic neurons (Kawaguchi et al. 1995). In the present study, three neuron subtypes were recorded, i.e., MS, FS, and PLTS neurons.

Table 2. *Properties of unitary IPSCs from MS/FS to MS neurons*

	Medium Spiny Neuron	*n*	Fast-Spiking Neuron	*n*
Connection rate to MS neuron, %	20.0	47/235	53.3†††	40/75
Latency, ms	1.2 ± 0.1	30	1.1 ± 0.2	25
Amplitude, pA	52.9 ± 10.3	30	109.4 ± 24.2*	25
Paired-pulse ratio	0.71 ± 0.04	30	0.75 ± 0.03	25
20-80% Rise time, ms	1.4 ± 0.2	30	1.1 ± 0.2	25
80-20% Decay time, ms	16.6 ± 1.0	30	16.8 ± 1.1	25
Half-duration, ms	10.6 ± 0.6	30	9.3 ± 0.5	25
τ_w, ms	12.9 ± 0.5	29	15.4 ± 2.0	24

Values are means ± SE. IPSC, inhibitory postsynaptic current. Weighted decay time constant (τ_w) is obtained from decay time constants of double exponential fitting curves (see MATERIALS AND METHODS). †††$P < 0.001$, χ^2-test; *$P < 0.05$, Student's *t*-test.

Pair-recorded MS neurons are shown in Fig. 1*A*. MS neurons were identified on the basis of their electrophysiological properties: *1*) a ramp depolarizing potential induced by a subthreshold step pulse injection, *2*) a temporal lag before repetitive firing, and *3*) adaptation of action potentials (Fig. 1*B*). In contrast, FS neurons showed large AHP amplitude and extremely high repetitive firing frequency without spike adaptation (Fig. 1*D*; Table 1). PLTS neurons were characterized by their low-threshold spike firing and large and persistent depolarization (data not shown). The population of recorded MS, FS, and PLTS neurons in this study was 97.6%, 2.2%, and 0.1%, respectively (n = 1,443). We found only two connections of MS→PLTS neurons, and therefore we did not include PLTS neurons in further analysis. Subthreshold responses and action potential kinetics of MS and FS neurons are summarized in Table 1.

Connection rate between MS→MS, MS→FS, and FS→MS pairs were 20.0%, 2.7%, and 53.3%, respectively (Table 2). Because only one FS→FS connection was found in this study, we did not include it for further analysis. Mutual connections were found in 1.7% of MS-MS pairs. Electrical synapses were rarely observed (0.4%) between MS-MS pairs. Typical examples of uIPSCs in MS→MS and FS→MS are shown in Fig. 1, *E* and *F*. The amplitude of uIPSCs in FS→MS was significantly larger than that in MS→MS connections ($P < 0.05$, Student's *t*-test; Table 2). On the other hand, other kinetics of uIPSCs for these connections, including the latency, PPR, 20–80% rise time, 80–20% decay time, half-duration, and decay time constant, were comparable (Fig. 1, *E* and *F*; Table 2). Application of 10 μM bicuculline almost completely diminished uIPSCs, suggesting that uIPSCs were predominantly

Fig. 1. Paired whole cell patch-clamp recording from medium spiny (MS)→MS and fast-spiking (FS)→MS neurons. *A*: example of fluorescence image of a pair of MS neurons recorded in nucleus accumbens (NAc) shell. Arrows show soma of each MS neuron. *B*, *top*: firing properties of a MS neuron in response to depolarizing square current pulses. *Bottom*: voltage responses of a MS neuron. Arrowheads and arrows show a ramp depolarizing potential and temporal lags before repetitive firing, respectively. Resting potential is shown on *left* of voltage traces. *C*: unitary inhibitory postsynaptic currents (uIPSCs) recorded from MS→MS neuron pair in control (*a*) and under application of bicuculline (10 μM), a $GABA_A$ receptor antagonist (*b*). *Top*: short depolarizing current pulses into presynaptic MS neurons, which elicit action potentials in the presynaptic MS neuron (*middle*). *Bottom*: uIPSCs responding to presynaptic action potentials. Ten consecutive traces are shown in gray lines, and averaged traces are shown in black. Note that uIPSCs are diminished by application of bicuculline. *D*: firing properties of a FS neuron responding to depolarizing square current pulses (*top*). Note high frequency of repetitive firing without adaptation (*bottom*). *E* and *F*: kinetics of uIPSC in MS→MS (*E*) and FS→MS (*F*) connections. Broken lines are fitted curves with double exponential function. τ, Weighted decay time constant (see MATERIALS AND METHODS).

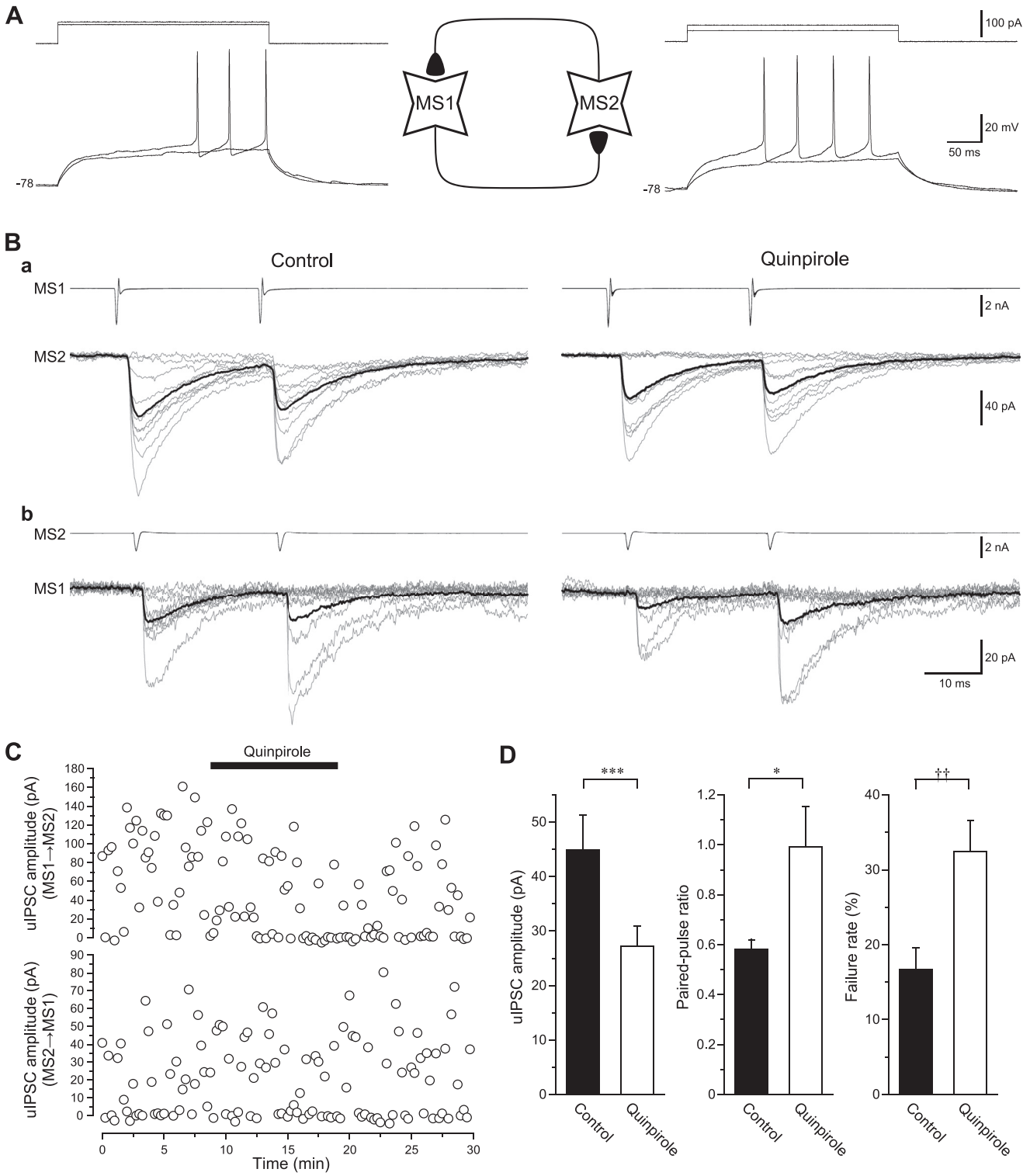

Fig. 2. Effects of quinpirole on uIPSCs recorded from MS→MS connections. *A*: scheme of mutual connection (MS1→MS2 and MS2→MS1) with subthreshold and firing properties of each MS neuron. Resting membrane potentials are shown on *left* of traces. *B*: effect of quinpirole (1 μM) on uIPSC of MS1→MS2 (*a*) and MS2→MS1 (*b*) connections. *Top* and *bottom*: presynaptic action currents and uIPSCs recorded from postsynaptic neurons, respectively. *Left* and *right*: traces in control and under quinpirole application, respectively. Ten consecutive traces are shown in gray lines, and averaged traces are shown in black. Note that quinpirole suppresses uIPSC amplitude in both connections. *C*: time courses of uIPSCs before, during, and after quinpirole application in MS1→MS2 and MS2→MS1 connections shown in *A* and *B*. *D*: summary of effects of quinpirole on uIPSC amplitude, paired-pulse ratio, and failure rate in MS→MS connections ($n = 29$). *$P < 0.05$, ***$P < 0.001$, paired *t*-test; ††$P < 0.01$, Wilcoxon test.

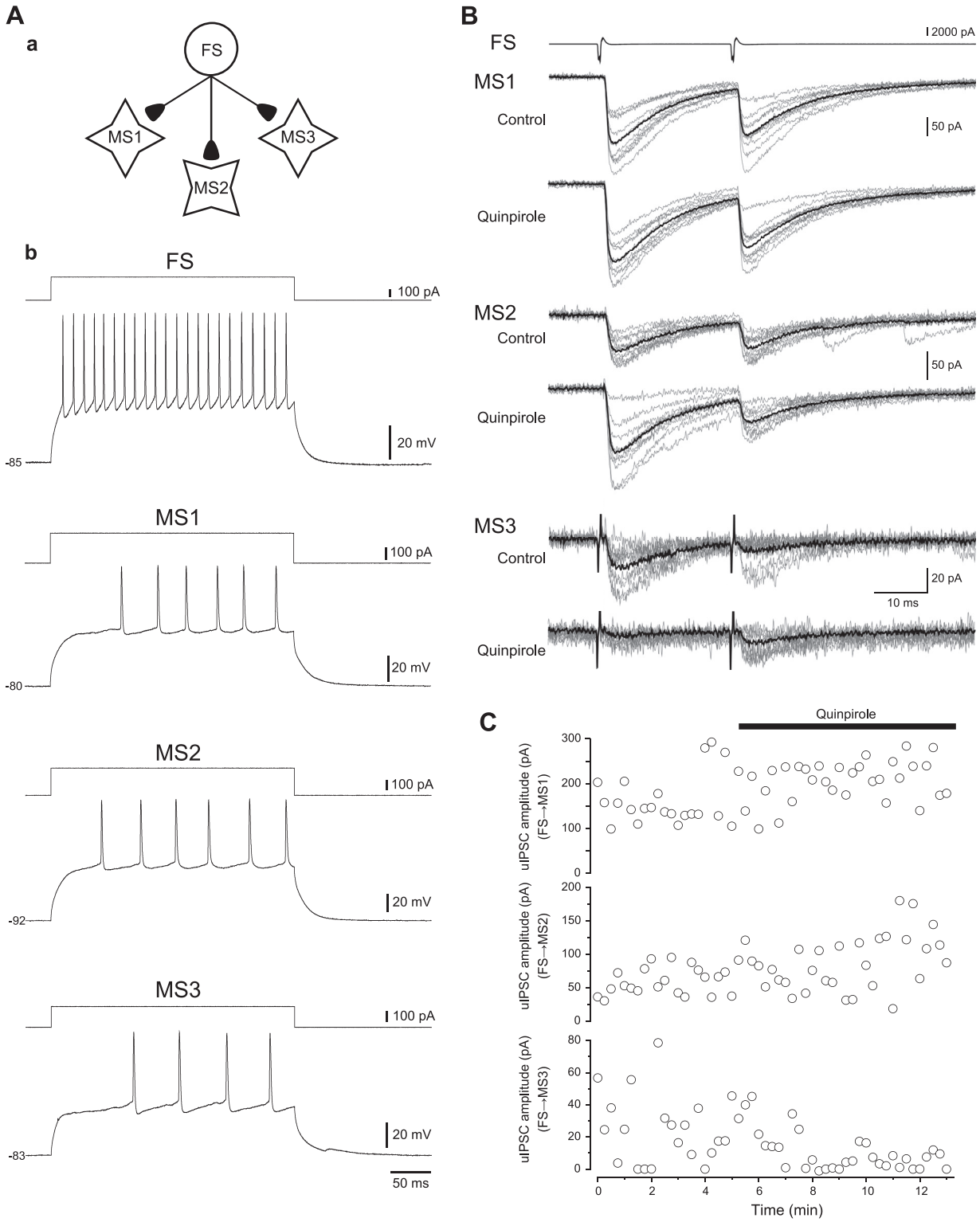

Fig. 3. Effects of quinpirole on uIPSCs in FS→MS connections. *A*, *a*: scheme of 3 MS neurons (MS1, MS2, and MS3) innervated by 1 FS neuron. *b*: Subthreshold and firing properties of each neuron. Resting membrane potentials are shown on *left* of traces. *B*: effect of quinpirole (1 μM) on uIPSC of FS→MS1/MS2/MS3 connections. *Top*: presynaptic action currents. *Bottom*: uIPSCs recorded from MS1, MS2, and MS3 neurons in control (upper) and under quinpirole application (lower). Ten consecutive traces are shown in gray lines, and averaged traces are shown in black. Note that quinpirole facilitates uIPSC amplitude in FS→MS1/MS2 connections, whereas it decreases uIPSC amplitude in FS→MS3 connections. *C*: time course of uIPSC amplitude on application of quinpirole in FS→MS connections shown in *A* and *B*.

mediated by $GABA_A$ receptors ($n = 8$ in MS→MS connections, Fig. 1*B*; $n = 3$ in FS→MS connections, data not shown).

Quinpirole suppresses MS-MS connection transmission presynaptically. Quinpirole is a dopamine D_2-like receptor agonist that nonselectively activates D_2, D_3, and D_4 receptors (Tang et al. 1994). Figure 2 shows a typical example of the effects of quinpirole on uIPSCs of MS→MS connections. Application of quinpirole (1 μM) reduced the amplitude of the first uIPSCs, in contrast to less effect on second uIPSC amplitude (Fig. 2*B*). The amplitude of the first uIPSCs was suppressed by quinpirole in 23 of 29 (79.3%) of MS→MS connections; in only 2 of 29 connections (6.9%) were uIPSCs facilitated by quinpirole. The remaining two connections were not substantially affected by quinpirole. Overall, quinpirole (1 μM) reduced the first uIPSC amplitude by 29.6 ± 5.9% ($n = 29$, $P < 0.001$, paired *t*-test). Suppression of uIPSCs by quinpirole was accompanied by increases in PPR (0.58 ± 0.04 to 0.99 ± 0.16; $n = 29$, $P < 0.05$, paired *t*-test) and failure rate (16.7 ± 3.0% to 32.4 ± 4.2%; $n = 29$, $P < 0.01$, Wilcoxon test), suggesting that quinpirole-induced suppression was likely to be mediated by presynaptic mechanisms.

Effects of quinpirole on uIPSCs in FS→MS connections. In contrast to the predominantly suppressive effects of quinpirole (1 μM) on MS→MS connections, FS→MS connections showed diverse effects of quinpirole. We analyzed 21 FS→MS connections with 14 presynaptic FS neurons. Eight connections (38.1%) showed quinpirole-induced facilitation of uIPSCs. On the other hand, five FS→MS connections (23.8%) showed uIPSC suppression by quinpirole. The other eight connections (38.1%) were not significantly affected by quinpirole. Mean amplitude of the first uIPSCs during application of 1 μM quinpirole ($n = 21$, 89.1 ± 15.5 pA) was comparable to that in controls (90.6 ± 15.2 pA; $P > 0.8$, paired *t*-test). The resting membrane potential of MS ($n = 29$) and FS cells ($n = 9$) was not significantly changed by application of quinpirole ($P > 0.1$, paired *t*-test).

Our quadruple whole cell recording, where one FS neuron innervates three MS neurons, showed that the presynaptic FS cell exhibited heterogeneous quinpirole-induced modulation of uIPSCs, i.e., two FS→MS connections (FS→MS1 and MS2) showed quinpirole-induced facilitation of uIPSCs, whereas one FS→MS (FS→MS3) connection showed suppression (Fig. 3). These results suggest that the effects of quinpirole on uIPSCs were different depending on the postsynaptic MS neurons, even though uIPSCs were generated by the same presynaptic FS cell.

CV analysis. To confirm whether the effects of quinpirole on uIPSCs in MS→MS or FS→MS connections are mediated by presynaptic mechanisms, we performed CV analysis (Bartos et al. 2001; Malinow and Tsien 1990). The mean and CV of the first uIPSC amplitude during quinpirole application were normalized by those in control, i.e., $CV^{-2}_{quinpirole}/CV^{-2}_{control}$ was plotted against $Mean_{quinpirole}/Mean_{control}$, respectively. If the plotted points are located at the identity line, this indicates that the effect of quinpirole is induced by presynaptic mechanisms including depletion of the vesicular pool (Stevens and Tsujimoto 1995).

Both in MS→MS and FS→MS connections, points were relatively broadly distributed, but most connections were located close to the identity line (Fig. 4). These results suggest that presynaptic mechanisms are involved at least in the part of the quinpirole-induced effects on uIPSCs obtained from MS→MS and FS→MS pairs, although we cannot exclude the possibility of postsynaptic mechanisms.

Cholinergic inputs do not contribute to quinpirole-induced uIPSC suppression in MS→MS connections. In addition to MS and FS neurons, cholinergic interneurons are another neuron subtype in the NAc (Kawaguchi 1993; Kawaguchi et al. 1995). Cholinergic interneurons are immunopositive for choline acetyltransferase and morphologically characterized by their giant somata (Kawaguchi 1993; Kawaguchi et al. 1995). They are characterized electrophysiologically by long-lasting AHP

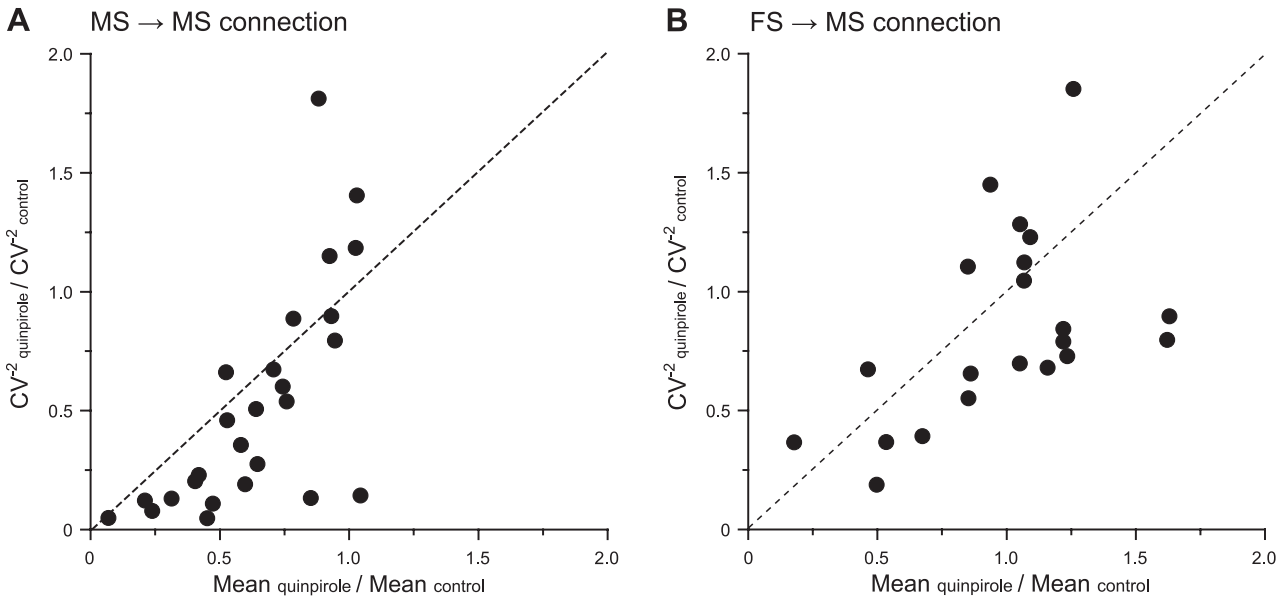

Fig. 4. Coefficient of variation (CV) analysis of effects of quinpirole on MS→MS (*A*) and FS→MS (*B*) connections. The inverse of the square of CV for the 1st uIPSCs under application of quinpirole is plotted against their mean amplitude; both CV and mean are normalized to the respective values of the 1st uIPSCs in controls. Lines of identity are indicated as dots.

and large hyperpolarization-activated cation current. In in vivo preparations, cholinergic interneurons show irregular firing at 2–10 Hz, suggesting that MS neurons receive tonic cholinergic inputs. Therefore, it is possible that quinpirole suppresses uIPSC amplitude by modulation of cholinergic inputs on MS neurons.

To examine this possibility, we analyzed the effects of quinpirole in combination with atropine and mecamylamine, nonselective muscarinic and nicotinic antagonists, respectively. Application of quinpirole (1 μM) under preapplication of atropine (1–10 μM) and mecamylamine (10 μM) significantly suppressed the amplitude of uIPSCs by 40.1 $\pm$ 9.4% ($n = 7$; $P < 0.01$, paired t-test). This reduction was equivalent to that with application of quinpirole alone, indicating that quinpirole-induced suppression of uIPSCs is less likely to be mediated by cholinergic modulation of MS neurons.

Sulpiride and nafadotride block quinpirole-induced suppression of MS→MS connections. To examine which receptor subtypes are involved in quinpirole-induced suppressive effects on the first uIPSC amplitude among D_2, D_3, and D_4 receptors, we examined the effect of quinpirole on uIPSCs under application of sulpiride or nafadotride.

Sulpiride is a relatively selective antagonist for D_2 receptors, although it has moderate affinity to D_3 receptors. Under preapplication of 1 μM sulpiride, quinpirole (1 μM) had little effect on uIPSC amplitude in MS→MS connections (96.0% of control; Fig. 5). Quinpirole did not significantly change PPR (0.68 $\pm$ 0.08 under sulpiride to 0.75 $\pm$ 0.08 with quinpirole; $n = 15$) or failure rate (34.0 $\pm$ 5.2% under sulpiride to 29.3 $\pm$ 5.8% with quinpirole; $n = 15$), as shown in Fig. 5*C*.

Nafadotride is a $D_{2/3}$ receptor antagonist with some preference for D_3 receptors; Audinot et al. (1998) reported that K_i is 0.52–0.88 nM for D_3 receptors and 5 nM for D_2 receptors. Similar to sulpiride, preapplication of nafadotride (10 μM) blocked quinpirole (1 μM)-induced uIPSC suppression (103.9% of controls; $n = 7$; Fig. 6). PPR was not significantly changed by quinpirole under application of nafadotride (0.57 $\pm$ 0.05 to 0.67 $\pm$ 0.11; $n = 7$). Failure rate was also little affected by quinpirole in combination with nafadotride (30.2 $\pm$ 7.2% to 28.0 $\pm$ 6.6%; $n = 7$).

These results suggest that $D_{2/3}$ receptors are involved in quinpirole-induced suppression of uIPSC amplitude in MS→MS connections.

PD128907 mimics quinpirole-induced suppression of uIPSCs between MS-MS neurons. Application of PD128907 (1 μM), a $D_{2/3}$ receptor agonist (Audinot et al. 1998; Bowery et al. 1996; van Vliet et al. 2000), invariably suppressed the amplitude of the first uIPSCs by 75.0 $\pm$ 7.0% ($n = 7$, $P <$

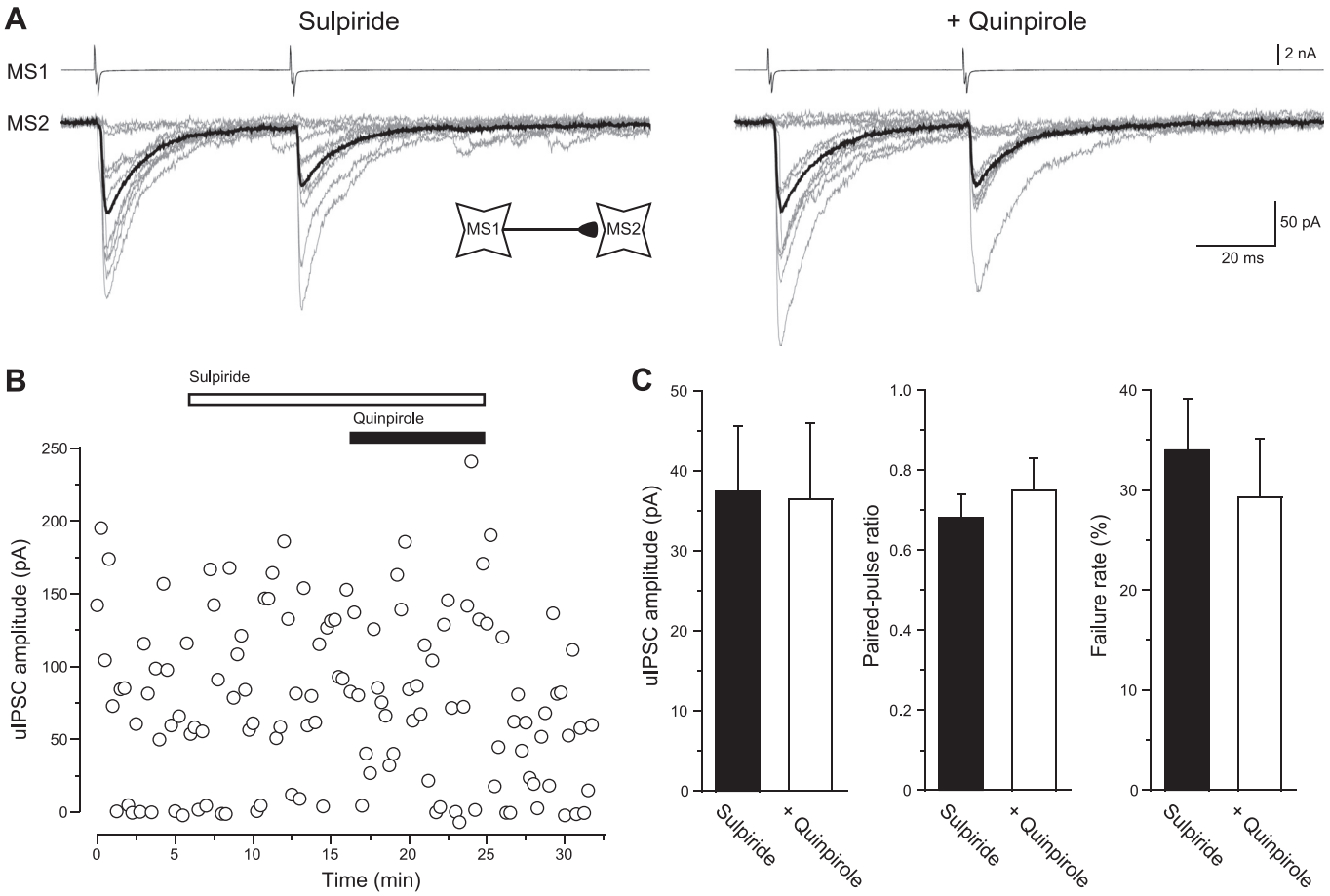

Fig. 5. Sulpiride (1 μM) blocks quinpirole-induced suppression of uIPSCs in MS→MS connections. *A*: typical traces under application of 1 μM sulpiride alone (*left*) and coapplication with 1 μM quinpirole (*right*). *Top*: presynaptic action currents (MS1). *Bottom*: uIPSCs recorded from postsynaptic neuron (MS2). Ten consecutive traces are shown in gray lines, and averaged traces are shown in black. *B*: time course of uIPSC amplitude on application of sulpiride and quinpirole shown in *A*. *C*: summary of uIPSC amplitude, paired-pulse ratio, and failure rate under application of sulpiride alone (filled bars) and coapplication with quinpirole (open bars). There is no significant difference between these 2 groups ($n = 15$).

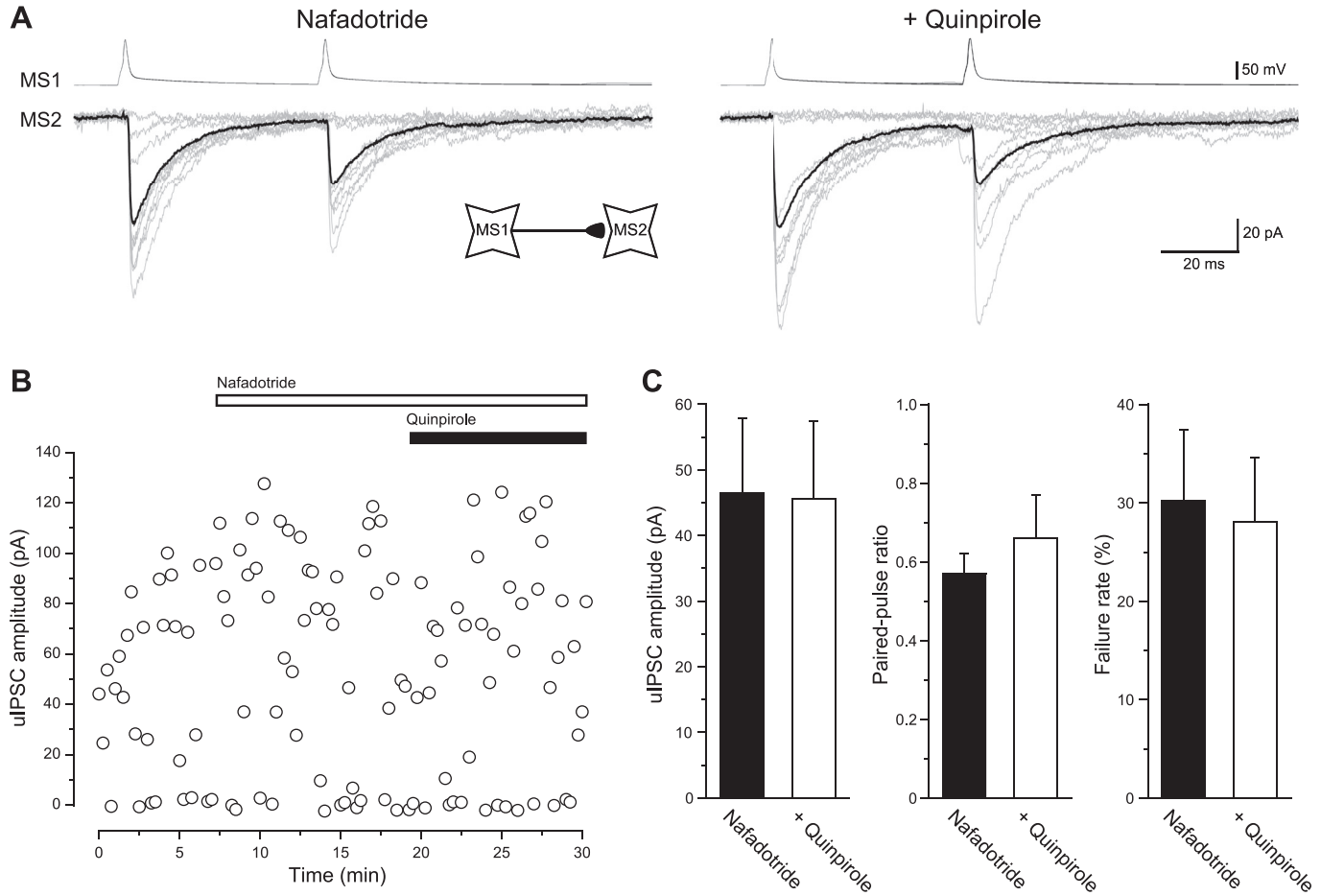

Fig. 6. Nafadotride (10 μM) blocks quinpirole-induced suppression of uIPSCs in MS→MS connections. *A*: typical traces under application of 10 μM nafadotride alone (*left*) and coapplication with 1 μM quinpirole (*right*). *Top*: presynaptic action currents (MS1). *Bottom*: uIPSCs recorded from postsynaptic neuron (MS2). Ten consecutive traces are shown in gray lines, and averaged traces are shown in black. *B*: time course of uIPSC amplitude on application of nafadotride and quinpirole shown in *A*. *C*: summary of uIPSC amplitude, paired-pulse ratio, and failure rate under application of nafadotride alone (filled bars) and coapplication with quinpirole (open bars). There is no significant difference between these 2 groups ($n = 7$).

0.05, paired *t*-test; Fig. 7). PD128907-induced suppression of uIPSCs was accompanied by significant increases in PPR (0.77 ± 0.13 to 1.25 ± 0.11; $n = 7$, $P < 0.05$, paired *t*-test) and failure rate (30.2 ± 7.2% to 43.6 ± 10.6%; $n = 7$, $P < 0.001$, Wilcoxon test).

These results support the idea described above that $D_{2/3}$ receptors are involved in quinpirole-induced suppression of uIPSC amplitude in MS→MS connections.

DISCUSSION

MS neurons in the NAc are innervated by GABAergic inhibitory inputs from FS neurons and recurrent collaterals from MS neurons themselves. MS→MS and FS→MS connections showed similar electrophysiological kinetics of uIPSCs, although their presynaptic firing properties were considerably different (Kawaguchi 1993; Taverna et al. 2007). A D_2-like receptor agonist, quinpirole, suppressed uIPSCs in MS→MS connections via $D_{2/3}$ receptors, whereas uIPSCs in FS→MS connections exhibited heterogeneous effects of quinpirole. CV analysis suggests that presynaptic mechanisms are involved in quinpirole-induced modulation of MS→MS and FS→MS connections.

Comparison of basic electrophysiological properties between MS and FS neuron-induced uIPSCs. As in the striatum (Kawaguchi 1993), GABAergic neurons in the NAc are classified into three subtypes by their anatomical and physiological properties, i.e., MS, FS, and PLTS neurons. Among these neurons, MS neurons are the major subtype; they occupy >90% of the total population of NAc neurons. In contrast, the population of FS neurons is reported to be much smaller: 11% in ventral striatum (Taverna et al. 2007). In the present study, these neuron subtypes were classified by electrophysiological properties, in accordance with previous reports (Kawaguchi 1993; Taverna et al. 2007). In terms of fundamental physiological properties of MS and FS neurons, our report extends previous studies by demonstrating that the amplitudes of uIPSC obtained from FS→MS connections are twice larger than those of MS→MS connections and the connection rate is much higher in FS→MS connections (53.3% vs. 20.0%) in the NAc. These findings are critical for estimating the impact of these inhibitory synapses on MS neurons.

Quinpirole differentially modulates MS→MS and FS→MS connections. If MS neurons without connections from adjacent MS neurons are impacted by similar excitatory postsynaptic potentials (EPSPs) from presynaptic glutamatergic neurons,

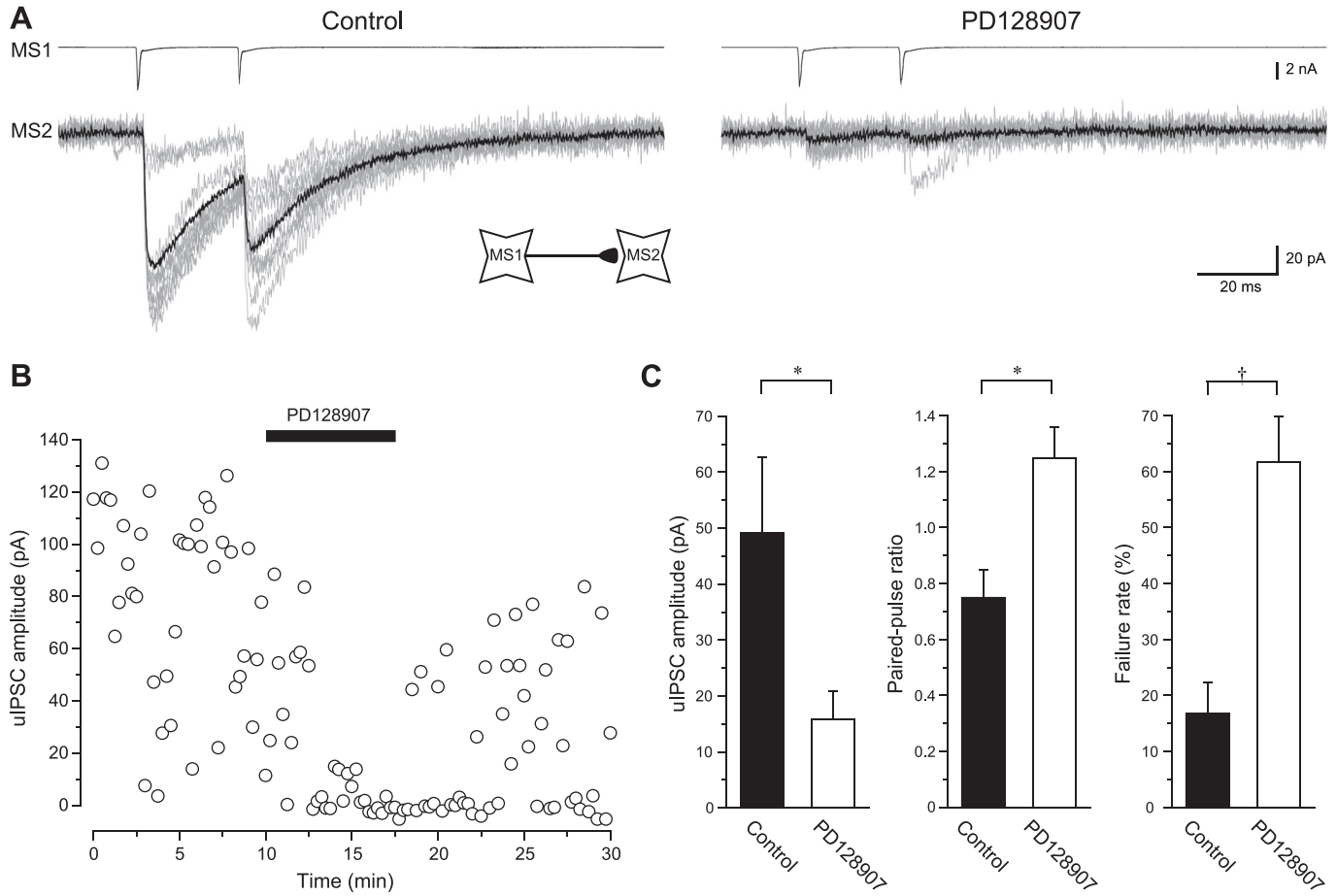

Fig. 7. Application of PD128907 (1 μM) mimics quinpirole-induced uIPSC suppression in MS→MS connections. *A*: effect of 1 μM PD128907 on uIPSC of MS1→MS2 connections. *Top* and *bottom*: presynaptic action currents and uIPSCs recorded from postsynaptic neurons, respectively. *Left* and *right*: traces in control and under PD128907 application, respectively. Ten consecutive traces are shown in gray lines, and averaged traces are shown in black. *B*: time courses of uIPSCs before, during, and after PD128907 application shown in *A*. *C*: summary of effects of PD128907 on uIPSC amplitude, paired-pulse ratio, and failure rate in MS→MS connections ($n = 7$). *$P < 0.05$, paired *t*-test; †$P < 0.05$, Wilcoxon test.

these MS neurons are likely to send inhibitory signals cooperatively so that neurons in projection sites such as the ventral pallidum receive potent inhibition. On the other hand, if MS neurons with connections are impacted similarly by EPSPs, initial activation of MS neurons suppresses surrounding MS neurons, i.e., lateral inhibition, and, as a result, inhibitory output is likely to be reduced. In the NAc, reciprocal connections between MS-MS neurons were found (Fig. 2; Taverna et al. 2005), suggesting that mutual connections between MS and MS neurons contribute to suppression of output signals. Therefore, uIPSC suppression via D_2-like receptor activation may increase output from the NAc. In contrast, FS→MS connections potently suppress many MS neurons, such that FS neurons effectively suppress outputs from MS neurons. The present finding of quinpirole-induced divergent effects on FS→MS connections suggests that FS neurons regulate outputs from the NAc in a complicated manner via D_2-like receptors.

Taken together with D_2-like receptor-dependent regulation of MS→MS and FS→MS connections, it is likely that D_2-like receptors increase the contrast of MS neuron activities depending on FS neuron activities: MS neurons increase output signals by reducing lateral inhibition during a dormant period of FS neuron activities, whereas a subpopulation of MS neurons are potently suppressed when FS neurons are activated (Guzmán et al. 2003).

Presynaptic $D_{2/3}$ receptors mediate quinpirole-induced suppression of uIPSCs in MS→MS connections. According to analyses of PPR, failure rate, and CV, the inhibitory effects of quinpirole on MS→MS connections are likely to be mediated via presynaptic mechanisms. Quinpirole is considered to be a nonselective agonist of D_2-like receptors, which include D_{2-4} receptors coupled to G_i protein (Stoof and Kebabian 1981). Both sulpiride, a relatively selective antagonist of D_2 receptors, and nafadotride, a relatively selective antagonist of D_3 receptors, diminished quinpirole-induced suppression of uIPSCs. We consider that these antagonists most likely block both D_2 and D_3 receptors, since sulpiride also binds to D_3 and nafadotride to D_2 receptors (Sokoloff et al. 1990). Although the results of sulpiride and nafadotride may exclude a contribution from D_4 receptors to uIPSC suppression by quinpirole (Audinot et al. 1998; Hernández et al. 2006), which is consistent with the finding that D_4 receptor expression is extremely low in the NAc (Tarazi et al. 1997), the present study did not show direct evidence that excludes the possibility of contribution of D_4 receptors to quinpirole-induced uIPSC suppression, and therefore this point should be examined with selective D_4 receptor agonists/antagonists in the future.

The result with PD128907, a $D_{2/3}$ receptor agonist (Pugsley et al. 1995), may suggest some greater contribution from D_3

receptors than from D_2 receptors (Chen et al. 2006; Hammad and Wagner 2006). Compared with the striatum, the NAc expresses more abundant D_3 receptors (Diaz et al. 2000; Murray et al. 1994; Sokoloff et al. 1990), suggesting important roles for NAc D_3 receptors in psychological disorders, including drug addiction and schizophrenia (Joyce and Millan 2005; Wilffert et al. 2005). The present results elucidate in part the mechanisms of these roles of D_3 receptors in the NAc: lateral inhibition of MS neurons is suppressed by D_3 receptor activation, which in turn facilitates output signals from the NAc.

Taverna et al. (2005) have reported presynaptic inhibition via D_1-like receptors in MS→MS connections in the NAc shell, using dual whole cell patch-clamp recordings. However, they have not investigated the inhibition via D_2-like receptors. Hjelmstad (2004) reported that evoked IPSCs in the NAc shell are inhibited via presynaptic D_1-like receptors but not D_2-like receptors. Nicola and Malenka (1997) also reported that activation of D_1-like receptors suppresses IPSCs recorded from MS neurons in the NAc core. They recorded evoked IPSCs by applying electrical stimulation via electrodes set extracellularly. Taken together with the present results of the contradictory actions of D_2-like receptors on MS→MS connections and FS→MS connections, a subpopulation of FS→MS connections that are facilitated by activating D_2-like receptors might mask the inhibitory effects on MS→MS synapses via D_2-like receptors. In addition, GABAergic afferents from the ventral pallidum might mask the effects on MS→MS synapses via D_2-like receptors. Furthermore, there is another possibility that dopaminergic modulations between the NAc core and shell could be different.

Functional considerations. NAc MS neurons send their GABAergic axons to the output structures of the basal ganglia, including the ventral pallidum and substantia nigra pars reticulata (Groenewegen et al. 1991). The projection neurons in both regions are GABAergic, and therefore D_2-like receptor-mediated facilitation of NAc MS neurons is likely to cause facilitation of neural activities in downstream structures, including thalamic nuclei, via disinhibition mechanisms. This working hypothesis may elaborate underlying mechanisms of D_2 receptor-mediated modulation of physiological functions in the NAc. These effects may be shared with D_1-like receptors (Taverna et al. 2005). Indeed, behavioral pharmacological studies have reported synergistic effects of D_1- and D_2-like receptors on oral dyskinesia (Cools et al. 1995). The present results may indicate a possible underlying mechanism for such oral dyskinesia.

To predict the functional roles of these connections, we have to consider the much higher firing rate of FS neurons, which will potently suppress MS neuron activity during the active state of FS neurons, in addition to the present static profiles of uIPSCs and anatomical features. Furthermore, a critical question is how excitatory and inhibitory inputs converge on MS and FS neurons. There are several possible mechanisms to explain quinpirole-induced differential modulation of uIPSCs between MS→MS and FS→MS connections. First, presynaptic voltage-gated calcium channels might be different in MS and FS neurons. Second, the involvement of D_2-like receptor subtypes might be different. If temporal activation patterns of MS and FS neurons are addressed, it could be possible to predict the dynamics of dopaminergic regulation of outputs via MS neurons more precisely, which would contribute to elucidation of the underlying mechanisms of dopaminergic drugs.

ACKNOWLEDGMENTS

We thank Dr. Kiyofumi Yamamoto for his excellent technical assistance, Dr. Satoshi Fujita for helpful discussion, and Prof. John L. Waddington for critical comments on the manuscript.

GRANTS

This work was supported by KAKENHI 20592188 to M. Kobayashi and 21890265 to S. Kohnomi; a Nihon University Joint Grant Research Grant to M. Kobayashi; The Promotion and Mutual Aid Corporation for Private Schools of Japan to N. Koshikawa and M. Kobayashi; the Uemura Foundation to M. Kobayashi; and a Grant for the Promotion of Multi-disciplinary Research Projects entitled "Translational Research Network on Orofacial Neurological Disorders" from the Japanese Ministry of Education, Culture, Sports, Science and Technology to N. Koshikawa and M. Kobayashi.

DISCLOSURES

No conflicts of interest, financial or otherwise, are declared by the author(s).

AUTHOR CONTRIBUTIONS

Author contributions: S.K. and M.K. performed experiments; S.K. and M.K. analyzed data; S.K., N.K., and M.K. interpreted results of experiments; S.K. and M.K. prepared figures; S.K. and M.K. drafted manuscript; S.K. and M.K. edited and revised manuscript; S.K., N.K., and M.K. approved final version of manuscript; N.K. and M.K. conception and design of research.

REFERENCES

Audinot V, Newman-Tancredi A, Gobert A, Rivet JM, Brocco M, Lejeune F, Gluck L, Desposte I, Bervoets K, Dekeyne A, Millan MJ. A comparative in vitro and in vivo pharmacological characterization of the novel dopamine D_3 receptor antagonists (+)-S 14297, nafadotride, GR 103,691 and U 99194. *J Pharmacol Exp Ther* 287: 187–197, 1998.

Bacci A, Rudolph U, Huguenard JR, Prince DA. Major differences in inhibitory synaptic transmission onto two neocortical interneuron subclasses. *J Neurosci* 23: 9664–9674, 2003.

Bartos M, Vida I, Frotscher M, Geiger JR, Jonas P. Rapid signaling at inhibitory synapses in a dentate gyrus interneuron network. *J Neurosci* 21: 2687–2698, 2001.

Bowery BJ, Razzaque Z, Emms F, Patel S, Freedman S, Bristow L, Kulagowski J, Seabrook GR. Antagonism of the effects of (+)-PD 128907 on midbrain dopamine neurones in rat brain slices by a selective D2 receptor antagonist L-741,626. *Br J Pharmacol* 119: 1491–1497, 1996.

Chen G, Kittler JT, Moss SJ, Yan Z. Dopamine D_3 receptors regulate $GABA_A$ receptor function through a phospho-dependent endocytosis mechanism in nucleus accumbens. *J Neurosci* 26: 2513–2521, 2006.

Cools AR, Miwa Y, Koshikawa N. Role of dopamine D_1 and D_2 receptors in the nucleus accumbens in jaw movements of rats: a critical role of the shell. *Eur J Pharmacol* 286: 41–47, 1995.

Czubayko U, Plenz D. Fast synaptic transmission between striatal spiny projection neurons. *Proc Natl Acad Sci USA* 99: 15764–15769, 2002.

Diaz J, Pilon C, Le Foll B, Gros C, Triller A, Schwartz JC, Sokoloff P. Dopamine D_3 receptors expressed by all mesencephalic dopamine neurons. *J Neurosci* 20: 8677–8684, 2000.

Di Chiara G. Nucleus accumbens shell and core dopamine: differential role in behavior and addiction. *Behav Brain Res* 137: 75–114, 2002.

Deutch AY, Cameron DS. Pharmacological characterization of dopamine systems in the nucleus accumbens core and shell. *Neuroscience* 46: 49–56, 1992.

Groenewegen HJ, Berendse HW, Meredith GE, Haber SN, Voorn P, Wolters JG, Lohman AH. Functional anatomy of the ventral, limbic system-innervated striatum. In: *The Mesolymbic Dopamine System: From Motivation to Action*, edited by Willner P, Scheel-Kruger J. Chichester, UK: Wiley, 1991. p. 19–59.

Guzmán JN, Hernández A, Galarraga E, Tapia D, Laville A, Vergara R, Aceves J, Bargas J. Dopaminergic modulation of axon collaterals interconnecting spiny neurons of the rat striatum. *J Neurosci* 23: 8931–8940, 2003.

Hammad H, Wagner JJ. Dopamine-mediated disinhibition in the CA1 region of rat hippocampus via D_3 receptor activation. *J Pharmacol Exp Ther* 316: 113–120, 2006.

Heimer L, Zahm DS, Churchill L, Kalivas PW, Wohltmann C. Specificity in the projection patterns of accumbal core and shell in the rat. *Neuroscience* 41: 89–125, 1991.

Hernández A, Ibáñez-Sandoval O, Sierra A, Valdiosera R, Tapia D, Anaya V, Galarraga E, Bargas J, Aceves J. Control of the subthalamic innervation of the rat globus pallidus by $D_{2/3}$ and D_4 dopamine receptors. *J Neurophysiol* 96: 2877–2888, 2006.

Hjelmstad GO. Dopamine excites nucleus accumbens neurons through the differential modulation of glutamate and GABA release. *J Neurosci* 24: 8621–8628, 2004.

Jongen-Rêlo AL, Voorn P, Groenewegen HJ. Immunohistochemical characterization of the shell and core territories of the nucleus accumbens in the rat. *Eur J Neurosci* 6: 1255–1264, 1994.

Joyce JN, Millan MJ. Dopamine D_3 receptor antagonists as therapeutic agents. *Drug Discov Today* 10: 917–925, 2005.

Kawaguchi Y. Physiological, morphological, and histochemical characterization of three classes of interneurons in rat neostriatum. *J Neurosci* 13: 4908–4923, 1993.

Kawaguchi Y, Wilson CJ, Augood SJ, Emson PC. Striatal interneurons: chemical, physiological and morphological characterization. *Trends Neurosci* 18: 527–535, 1995.

Kobayashi M, Hamada T, Kogo M, Yanagawa Y, Obata K, Kang Y. Developmental profile of $GABA_A$-mediated synaptic transmission in pyramidal cells of the somatosensory cortex. *Eur J Neurosci* 28: 849–861, 2008.

Koós T, Tepper JM. Inhibitory control of neostriatal projection neurons by GABAergic interneurons. *Nat Neurosci* 2: 467–472, 1999.

Koshikawa N, Koshikawa F, Tomiyama K, Kikuchi de Beltrán K, Kamimura F, Kobayashi M. Effects of dopamine D_1 and D_2 agonists and antagonists injected into the nucleus accumbens and globus pallidus on jaw movements of rats. *Eur J Pharmacol* 182: 375–380, 1990.

Koshikawa N, Miwa Y, Adachi K, Kobayashi M, Cools AR. Behavioural effects of 7-OH-DPAT are solely due to stimulation of dopamine D_2 receptors in the shell of the nucleus accumbens; jaw movements. *Eur J Pharmacol* 308: 227–234, 1996.

Koyanagi Y, Yamamoto K, Oi Y, Koshikawa N, Kobayashi M. Presynaptic interneuron subtype- and age-dependent modulation of GABAergic synaptic transmission by β-adrenoceptors in rat insular cortex. *J Neurophysiol* 103: 2876–2888, 2010.

Lu XY, Ghasemzadeh MB, Kalivas PW. Expression of D_1 receptor, D_2 receptor, substance P and enkephalin messenger RNAs in the neurons projecting from the nucleus accumbens. *Neuroscience* 82: 767–780, 1998.

Malinow R, Tsien RW. Presynaptic enhancement shown by whole-cell recordings of long-term potentiation in hippocampal slices. *Nature* 346: 177–180, 1990.

Morgane PJ, Galler JR, Mokler DJ. A review of systems and networks of the limbic forebrain/limbic midbrain. *Prog Neurobiol* 75: 143–160, 2005.

Murray AM, Ryoo HL, Gurevich E, Joyce JN. Localization of dopamine D_3 receptors to mesolimbic and D_2 receptors to mesostriatal regions of human forebrain. *Proc Natl Acad Sci USA* 91: 11271–11275, 1994.

Nicola SM, Kombian SB, Malenka RC. Psychostimulants depress excitatory synaptic transmission in the nucleus accumbens via presynaptic D1-like dopamine receptors. *J Neurosci* 16: 1591–1604, 1996.

Nicola SM, Malenka RC. Dopamine depresses excitatory and inhibitory synaptic transmission by distinct mechanisms in the nucleus accumbens. *J Neurosci* 17: 5697–5710, 1997.

Nicola SM. The nucleus accumbens as part of a basal ganglia action selection circuit. *Psychopharmacology (Berl)* 191: 521–550, 2007.

Pennartz CM, Kitai ST. Hippocampal inputs to identified neurons in an in vitro slice preparation of the rat nucleus accumbens: evidence for feed-forward inhibition. *J Neurosci* 11: 2838–2847, 1991.

Pennartz CM, Dolleman-Van der Weel MJ, Kitai ST, Lopes da Silva FH. Presynaptic dopamine D1 receptors attenuate excitatory and inhibitory limbic inputs to the shell region of the rat nucleus accumbens studied in vitro. *J Neurophysiol* 67: 1325–1334, 1992.

Pennartz CM, Groenewegen HJ, Lopes da Silva FH. The nucleus accumbens as a complex of functionally distinct neuronal ensembles: an integration of behavioural, electrophysiological and anatomical data. *Prog Neurobiol* 42: 719–761, 1994.

Prinssen EP, Balestra W, Bemelmans FF, Cools AR. Evidence for a role of the shell of the nucleus accumbens in oral behavior of freely moving rats. *J Neurosci* 14: 1555–1562, 1994.

Pugsley TA, Davis MD, Akunne HC, MacKenzie RG, Shih YH, Damsma G, Wikstrom H, Whetzel SZ, Georgic LM, Cooke LW, Demattos SB, Corbin AE, Glase SA, Wise LD, Dijkstra D, Heffner TG. Neurochemical and functional characterization of the preferentially selective dopamine D_3 agonist PD 128907. *J Pharmacol Exp Ther* 275: 1355–1366, 1995.

Sharp T, Zetterstrom T, Ljungberg T, Ungerstedt U. A direct comparison of amphetamine-induced behaviours and regional brain dopamine release in the rat using intracerebral dialysis. *Brain Res* 401: 322–330, 1987.

Shinonaga Y, Takada M, Mizuno N. Topographic organization of collateral projections from the basolateral amygdaloid nucleus to both the prefrontal cortex and nucleus accumbens in the rat. *Neuroscience* 58: 389–397, 1994.

Sibley DR, Monsma FJ Jr, Shen Y. Molecular neurobiology of dopaminergic receptors. *Int Rev Neurobiol* 35: 391–415, 1993.

Sokoloff P, Giros B, Martres MP, Bouthenet ML, Schwartz JC. Molecular cloning and characterization of a novel dopamine receptor (D_3) as a target for neuroleptics. *Nature* 347: 146–151, 1990.

Stevens CF, Tsujimoto T. Estimates for the pool size of releasable quanta at a single central synapse and for the time required to refill the pool. *Proc Natl Acad Sci USA* 92: 846–849, 1995.

Stoof JC, Kebabian JW. Opposing roles for D-1 and D-2 dopamine receptors in efflux of cyclic AMP from rat neostriatum. *Nature* 294: 366–368, 1981.

Tang L, Todd RD, Heller A, O'Malley KL. Pharmacological and functional characterization of D_2, D_3 and D_4 dopamine receptors in fibroblast and dopaminergic cell lines. *J Pharmacol Exp Ther* 268: 495–502, 1994.

Tarazi FI, Kula NS, Baldessarini RJ. Regional distribution of dopamine D_4 receptors in rat forebrain. *Neuroreport* 8: 3423–3426, 1997.

Taverna S, van Dongen YC, Groenewegen HJ, Pennartz CM. Direct physiological evidence for synaptic connectivity between medium-sized spiny neurons in rat nucleus accumbens in situ. *J Neurophysiol* 91: 1111–1121, 2004.

Taverna S, Canciani B, Pennartz CM. Dopamine D_1-receptors modulate lateral inhibition between principal cells of the nucleus accumbens. *J Neurophysiol* 93: 1816–1819, 2005.

Taverna S, Canciani B, Pennartz CM. Membrane properties and synaptic connectivity of fast-spiking interneurons in rat ventral striatum. *Brain Res* 1152: 49–56, 2007.

Taverna S, Ilijic E, Surmeier DJ. Recurrent collateral connections of striatal medium spiny neurons are disrupted in models of Parkinson's disease. *J Neurosci* 28: 5504–5512, 2008.

Tepper JM, Koós T, Wilson CJ. GABAergic microcircuits in the neostriatum. *Trends Neurosci* 27: 662–669, 2004.

Tepper JM, Wilson CJ, Koós T. Feedforward and feedback inhibition in neostriatal GABAergic spiny neurons. *Brain Res Rev* 58: 272–281, 2008.

van Vliet LA, Serpa KA, Meltzer LT, Heffner TG, Wise LD. Synthesis and pharmacological evaluation of thiopyran analogues of the dopamine D_3 receptor-selective agonist (4aR,10bR)-(+)-*trans*-3,4,4a,10b-tetrahydro-4-n-2H,5H-[1]benzopyrano[4,3-b]-1,4-oxazin-9-ol (PD 128907). *J Med Chem* 43: 2871–2882, 2000.

Wilffert B, Zaal R, Brouwers JR. Pharmacogenetics as a tool in the therapy of schizophrenia. *Pharm World Sci* 27: 20–30, 2005.

Yamamoto K, Koyanagi Y, Koshikawa N, Kobayashi M. Postsynaptic cell type-dependent cholinergic regulation of GABAergic synaptic transmission in rat insular cortex. *J Neurophysiol* 104: 1933–1945, 2010.

Zahm DS, Brog JS. On the significance of subterritories in the "accumbens" part of the rat ventral striatum. *Neuroscience* 50: 751–767, 1992.